

Supplementary Materials

Table S1 contains data on measured ^{10}Be concentrations conducted for this study. Figures S1-S12 show the MCMC chains of accepted parameter combinations for each retreat scenario, for each transect, and likelihood-weighted histograms for each parameter from which parameter estimates and uncertainties were determined (Table S2-S3). The results of each MCMC chain are shown in Figures S1-S12. These figures show the parameter values accepted by the chains over the 200k iterations simulated, and the resulting likelihood-weighted probability density and cumulative density plots used to estimate the most likely parameter values and uncertainty.

At Hope Gap, similar likelihoods were obtained for the single retreat rate, linear change in retreat rate, and a step change in retreat rate scenarios. At Beachy Head, a step change in retreat rate performs significantly better than either a constant retreat rate or gradual change in retreat rate. There is a trade-off between ε_2 and t such that a more recent change time coupled to a higher retreat rate produces similar profiles to an older change time and lower recent retreat rate (Figure S13). Thus, we are unable to constrain whether a more rapid retreat rate initiated more recently, or a slightly slower rate further back in time. As a result of this, there appear to be multiple attractor locations in the parameter space depending on ε_2 and t .

Table S1: ^{10}Be sample and concentration data.

Sample ID	Location (British Nat. Grid)		Distance from Cliff (m)	Elevation above ordnance datum (m)	Mass of quartz dissolved (g)	Mass of carrier added (g)*	Measured $^{10}\text{Be}/^9\text{Be}$ ratio ($\times 10^{-14}$)	$\pm 1\sigma$ AMS analytical uncertainty $^{10}\text{Be}/^9\text{Be}$ ratio ($\times 10^{-14}$)	Background-corrected Concentration ^{10}Be ($\times 10^3$ atoms g^{-1})**	$\pm 1\sigma$ AMS Analytical uncertainty ($\times 10^3$ atoms g^{-1})	Inheritance-corrected ^{10}Be *** ($\times 10^3$ atoms g^{-1})	\pm **** ($\times 10^3$ atoms g^{-1})
	Easting (m)	Northing (m)										
HG-03	551032	97178	216.5	-1.54	65.737	0.973	4.825	0.139	9.31	0.28	5.11	0.39
HG-05	551079	97093	313.5	-2.98	65.862	0.972	4.362	0.124	8.35	0.25	4.15	0.37
HG-06	551025	97133	258.7	-1.24	59.316	0.973	4.881	0.185	10.44	0.42	6.25	0.49
HG-07	551021	97165	226.8	-2.01	64.127	0.974	4.363	0.130	8.59	0.27	4.39	0.38
HG-08	551017	97216	177.8	-0.52	57.464	0.974	4.539	0.115	9.99	0.27	5.80	0.38
HG-09	551004	97198	190.1	-0.64	68.858	0.971	5.995	0.190	11.12	0.37	6.92	0.45
HG-10a	551014	97248	146.6	-0.11	61.812	0.972	4.341	0.176	8.85	0.38	4.65	0.46
HG-10b	551012	97249	144.9	-0.11	56.102	0.972	3.909	0.148	8.73	0.35	4.53	0.44
HG-11	551009	97283	111.3	0.17	53.048	0.971	2.989	0.095	6.93	0.24	2.73	0.36
HG-12	551003	97309	84.6	0.42	50.808	0.971	7.578	0.166	19.19	0.43	14.99	0.51
HG-13	550998	97333	61.0	0.87	56.553	0.970	2.658	0.096	5.71	0.23	1.52	0.35
HG-14	550992	97342	49.8	1.16	50.353	0.971	2.120	0.088	5.01	0.24	0.82	0.36
HG-15	550906	97384	-5.0	5.0	53.321	0.970	1.905	0.106	4.20	0.27	0	0.38
CFG1405A	-	-	-	-	-	-	0.207	0.130	-	-	-	-
CFG1405B	-	-	-	-	-	-	0.217	0.106	-	-	-	-
BH-05	555919	95501	79.3	-0.50	52.287	0.975	1.901	0.097	3.26	0.57	0.36	0.78
BH-13	555939	95516	57.8	0.37	61.283	0.973	1.954	0.136	2.87	0.53	0	0.75
BH-14	555913	95477	103.7	-0.53	54.364	0.976	2.015	0.107	3.40	0.56	0.52	0.77
BH-15	555892	95463	124.3	-0.94	41.660	0.974	1.811	0.075	3.77	0.69	0.90	0.87
BH-16	555893	95441	144.8	-1.21	41.172	0.974	2.004	0.114	4.44	0.75	1.57	0.92
BH-17	555877	95427	162.9	-1.81	49.262	0.970	5.828	0.211	13.97	0.78	11.09	0.95
BH-18	555870	95413	178.6	-1.58	45.440	0.972	3.848	0.115	9.39	0.68	6.52	0.86
BH-19	555854	95402	195.4	-2.35	42.785	0.972	2.644	0.121	6.24	0.73	3.37	0.90
BH-20	555842	95388	212.7	-2.29	52.843	0.972	5.617	0.210	12.51	0.73	9.64	0.90
BH-21	555814	95382	227.9	-2.77	52.663	0.971	2.968	0.097	5.88	0.57	3.01	0.77
BH-22	555805	95366	246.7	-2.90	50.237	0.972	3.013	0.180	6.29	0.72	3.42	0.89
BH-23	555813	95349	259.4	-3.55	52.866	0.972	3.014	0.125	5.98	0.60	3.11	0.80
CFG1410A	-	-	-	-	-	-	0.770	0.059	-	-	-	-
CFG1410B	-	-	-	-	-	-	0.485	0.074	-	-	-	-

* Carrier concentration $204 \mu\text{g Be g}^{-1}$.** Normalized to the 07KNSTD3110 standard with an assumed ratio of 2.85×10^{-12} . Values corrected for chemistry background using average and standard deviation of two full chemistry blanks processed in each batch with errors in sample and blank propagated in quadrature.

*** All HG samples were corrected for inheritance with HG-15, which was a fully shielded sample taken from a cave in the cliff. BH samples were corrected for inheritance with BH-05, assuming little accumulation of CRNs.

**** Error propagated as $\sigma_c = \sqrt{\sigma_a^2 + \sigma_b^2}$ where σ_a is the error of the measured concentration, σ_b is the error of the measured concentration used for the correction (HG-15/BH-05).

Table S2: Results of Monte Carlo simulations for Hope Gap transect

Parameters	Retreat Rate Scenario		
	1. Constant	2. Step Change	3. Linear Change
Retreat Rate 1 (cm yr ⁻¹)	5.4 ^{+0.3} _{-0.3}	5.7 ^{+0.3} _{-0.3}	17.8 ^{+2.8} _{-2.7}
Retreat Rate 2 (cm yr ⁻¹)	-	1.3 ^{+1.1} _{-0.3}	3.7 ^{+1.0} _{-1.0}
Change Time (yr BP)	-	308 ⁺¹³⁵ ₋₁₀₀	-
Beach Width (m)	43.3 ^{+2.1} _{-1.0}	47.0 ^{+1.6} _{-1.0}	40.8 ^{+4.8} _{-5.6}
-log(L)	41.1	33.7	40.5

Table S3: Results of Monte Carlo simulations for Beachy Head transect.

Parameters	Retreat Rate Scenario		
	1. Constant	2. Step Change	3. Linear Change
Retreat Rate 1 (cm yr ⁻¹)	4.7 ^{+0.4} _{-0.4}	2.6 ^{+0.2} _{-0.2}	1.8 ^{+1.1} _{-0.8}
Retreat Rate 2 (cm yr ⁻¹)	-	30.4 ^{+8.3} _{-10.6}	6.3 ^{+0.7} _{-0.8}
Change Time (yr BP)	-	293 ⁺¹⁷⁰ ₋₈₀	-
Beach Width (m)	42.7 ^{+3.0} _{-3.6}	17.7 ^{+3.7} _{-5.5}	35.5 ^{+3.6} _{-4.4}
-log(L)	121.7	83.7	116.9

Supplementary Figures

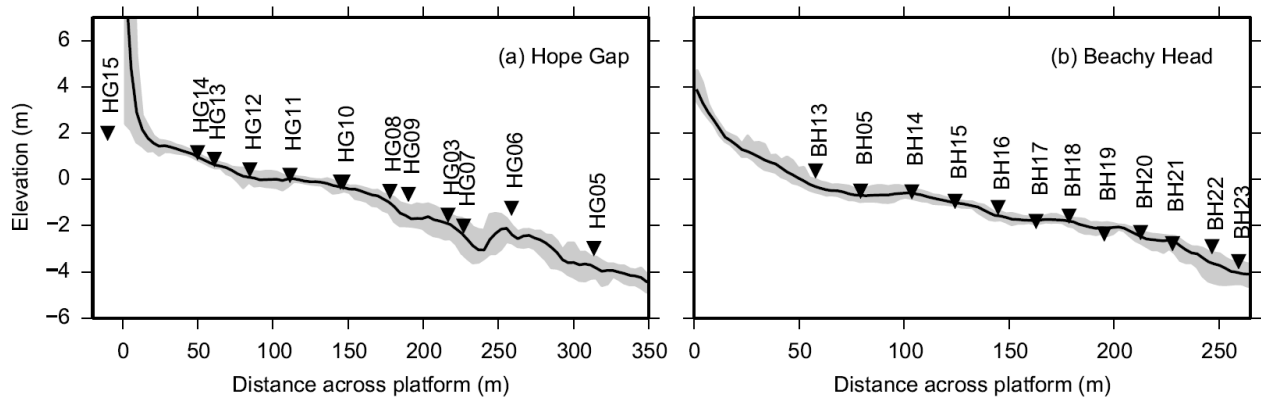


Figure S1: Swath profiles of platform morphology from stitched LiDAR and multibeam elevation data (data courtesy of the Channel Coast Observatory; www.channelcoast.org) and sample locations (black triangles) for (a) Hope Gap and (b) Beachy Head transects. Black lines are mean elevation within a 10 m wide swath, grey shaded region shows the range of elevations within the swath.

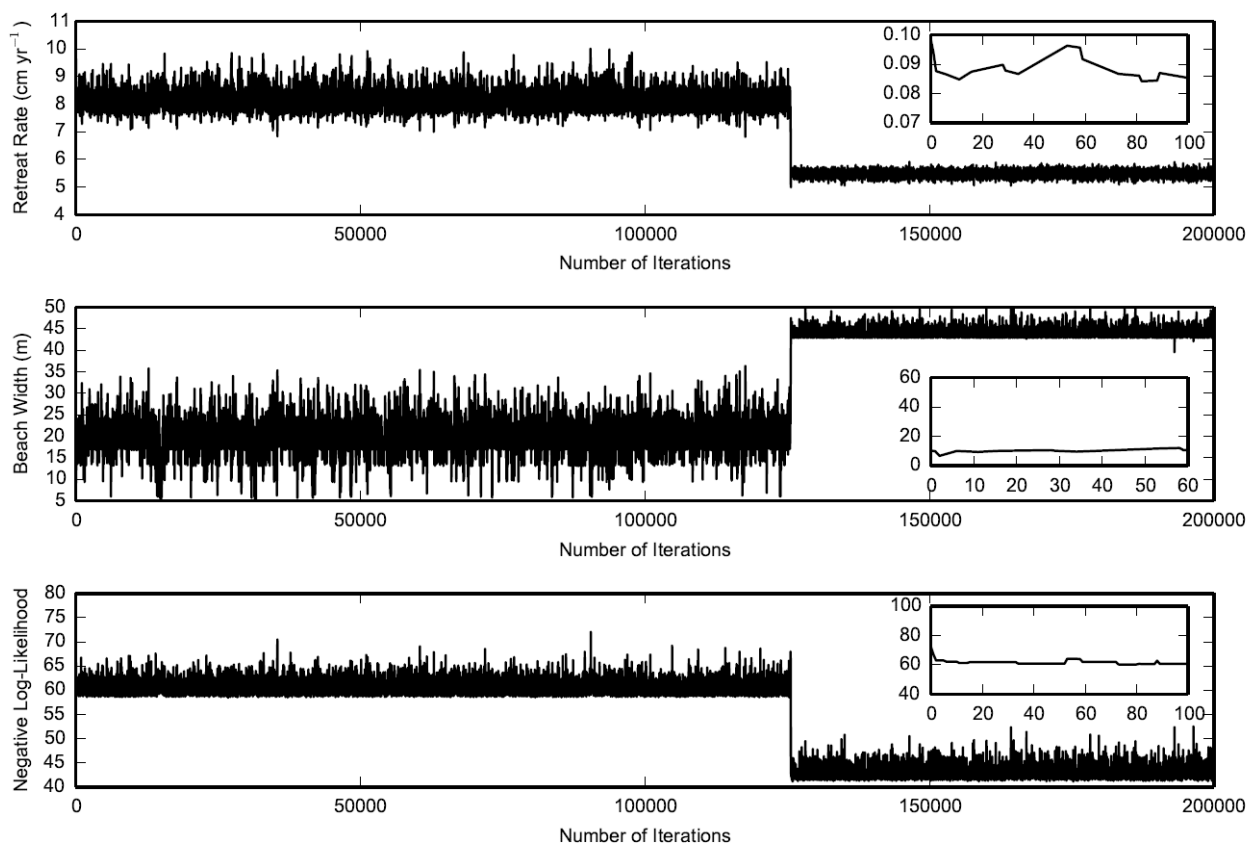


Figure S2: MCMC results for accepted parameters for Hope Gap using a single retreat rate. There were two attractor states in the parameter space with a switch to the more likely state occurring after $\sim 125\text{k}$ iterations in the chain. Inset plots show burn in period.

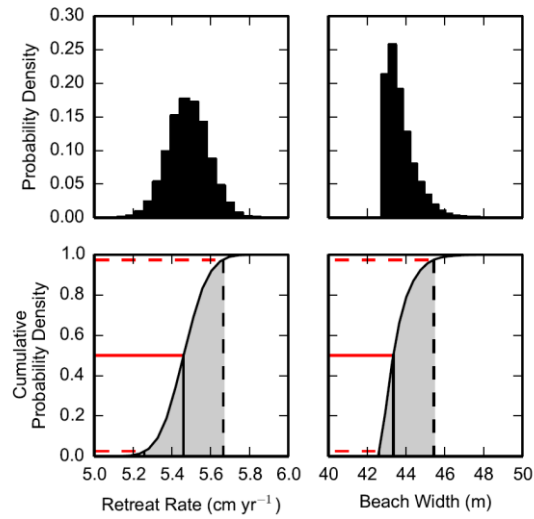


Figure S3: Likelihood weighted histograms giving parameter estimates for Hope Gap from MCMC inversion for single retreat rate scenario. Most likely values taken as the median with 95% confidence intervals. Note these plots include all data from Figure S2.

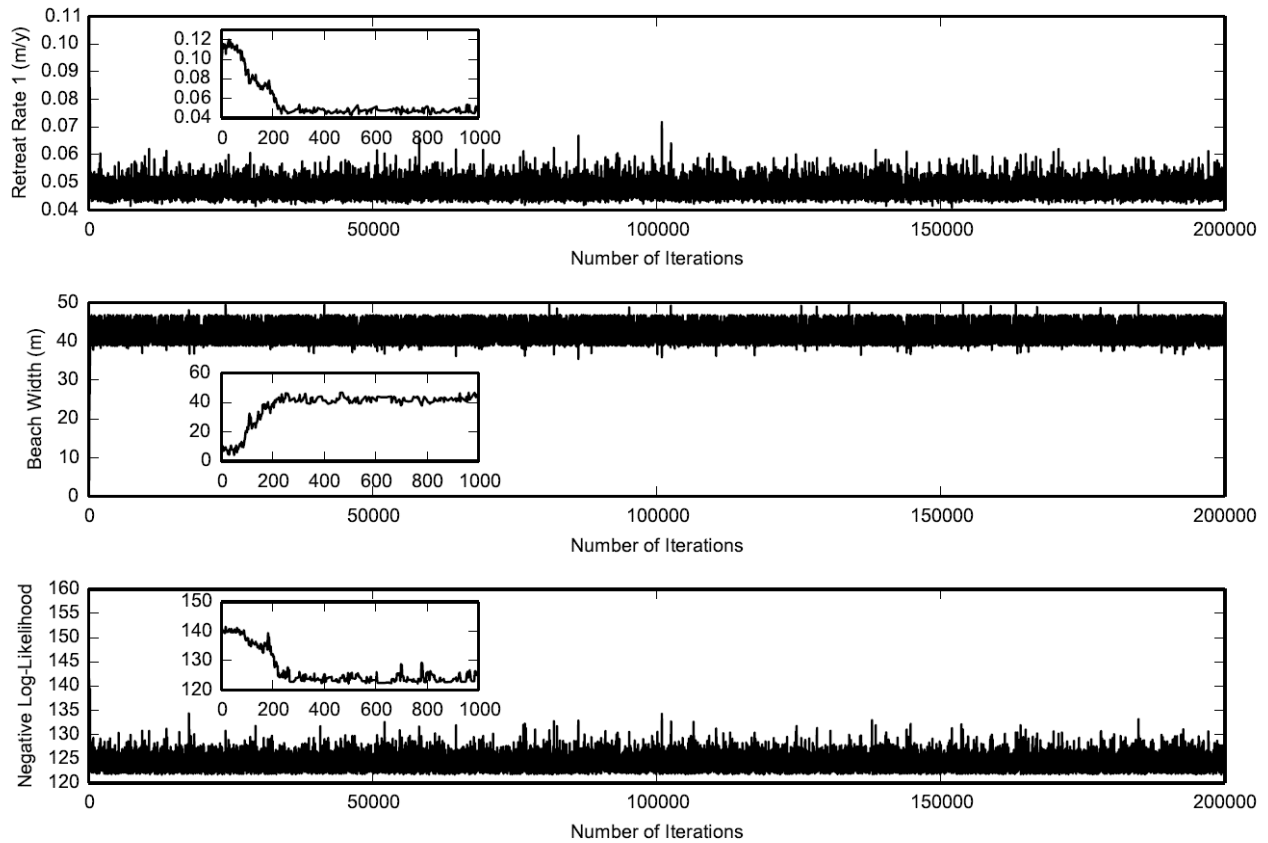


Figure S4: MCMC results for accepted parameters for Beachy Head using a single retreat rate. Inset plots show burn in period.

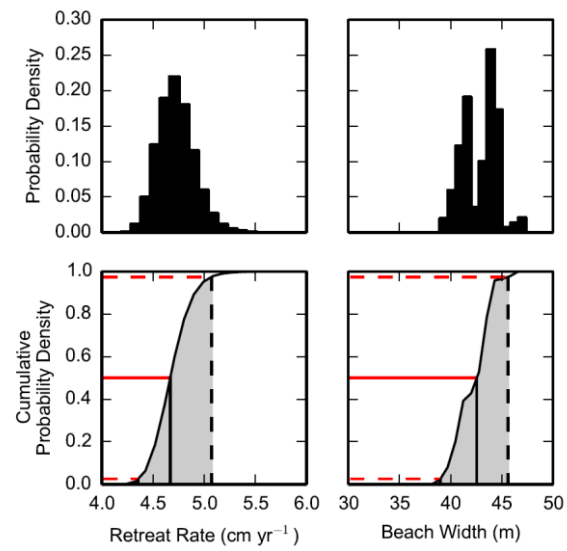


Figure S5: Likelihood weighted histograms giving parameter estimates for Beachy Head from MCMC inversion for single retreat rate scenario. Most likely values taken as the median with 95% confidence intervals. Note these plots include all data from Figure S4.

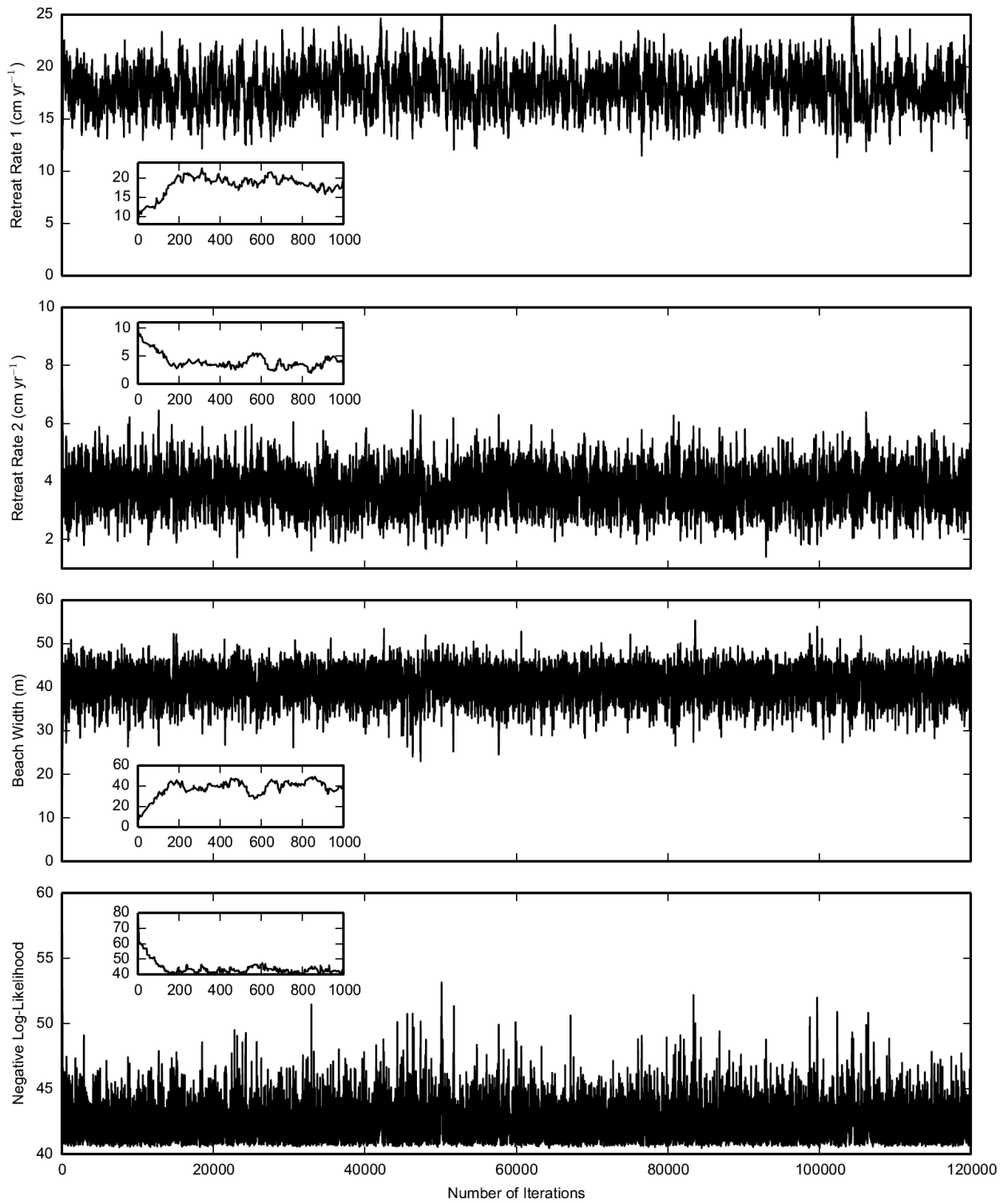


Figure S6: MCMC results for accepted parameters for Hope Gap using a linearly changing retreat rate. Inset plots show burn in period.

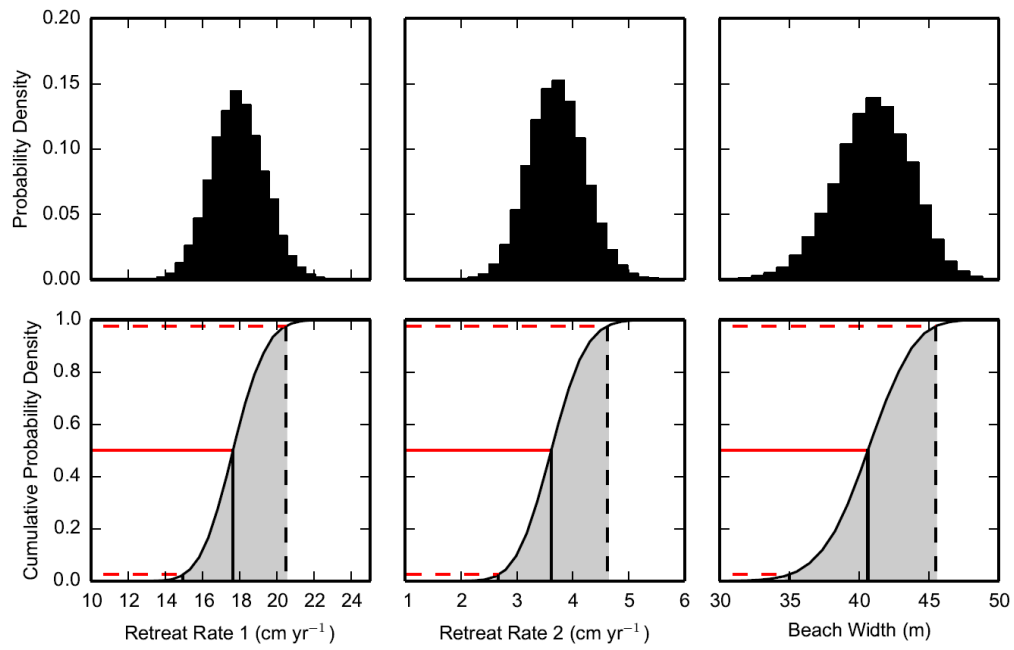


Figure S7: Likelihood weighted histograms giving parameter estimates for Hope Gap from MCMC inversion for linearly changing retreat rate scenario. Most likely values taken as the median with 95% confidence intervals. Note these plots include all data from Figure S6.

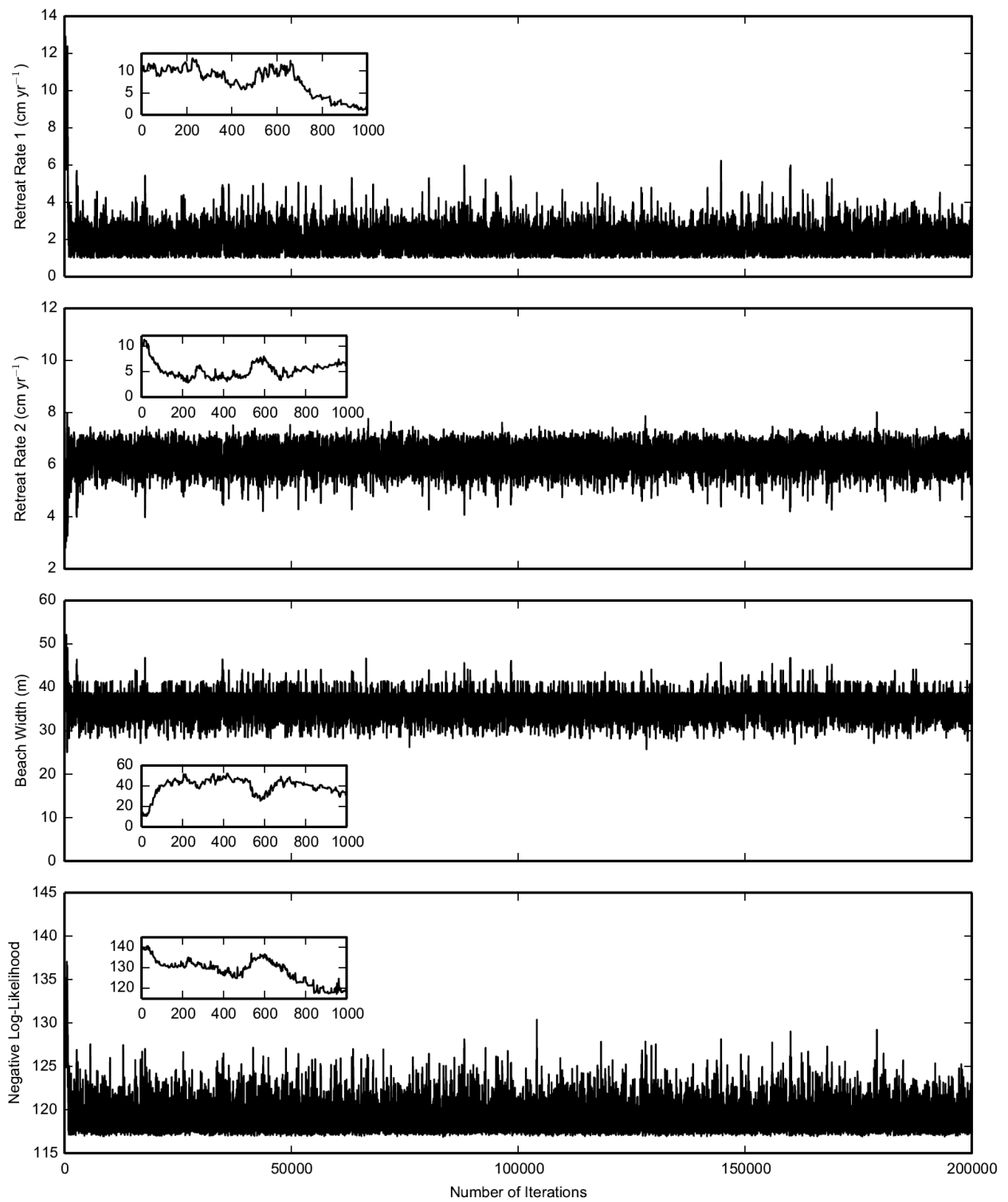


Figure S8: MCMC results for accepted parameters for Beachy Head using a linearly changing retreat rate. Inset plots show burn in period.

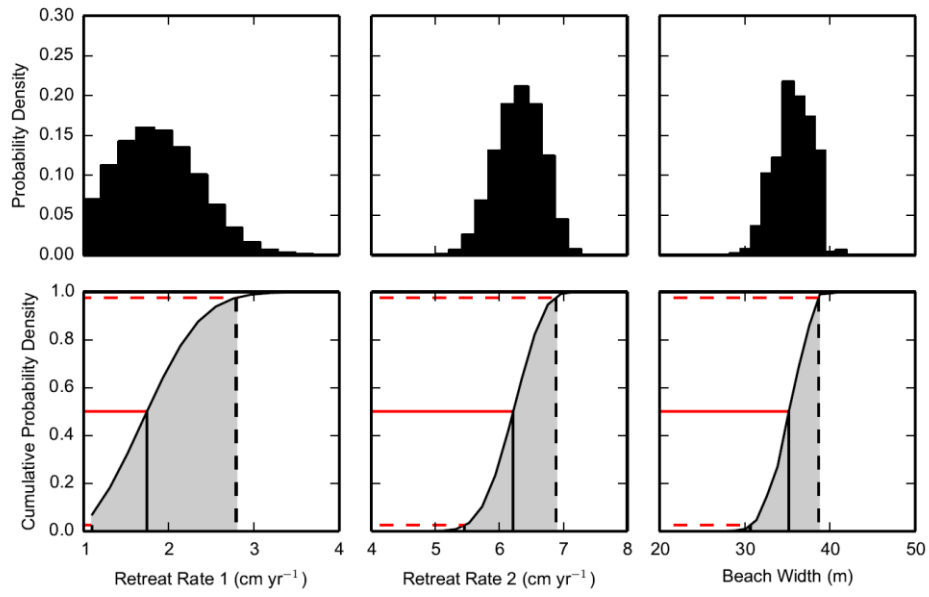


Figure S9: Likelihood weighted histograms giving parameter estimates for Hope Gap from MCMC inversion for linearly changing retreat rate scenario. Most likely values taken as the median with 95% confidence intervals. Note these plots include all data from Figure S8.

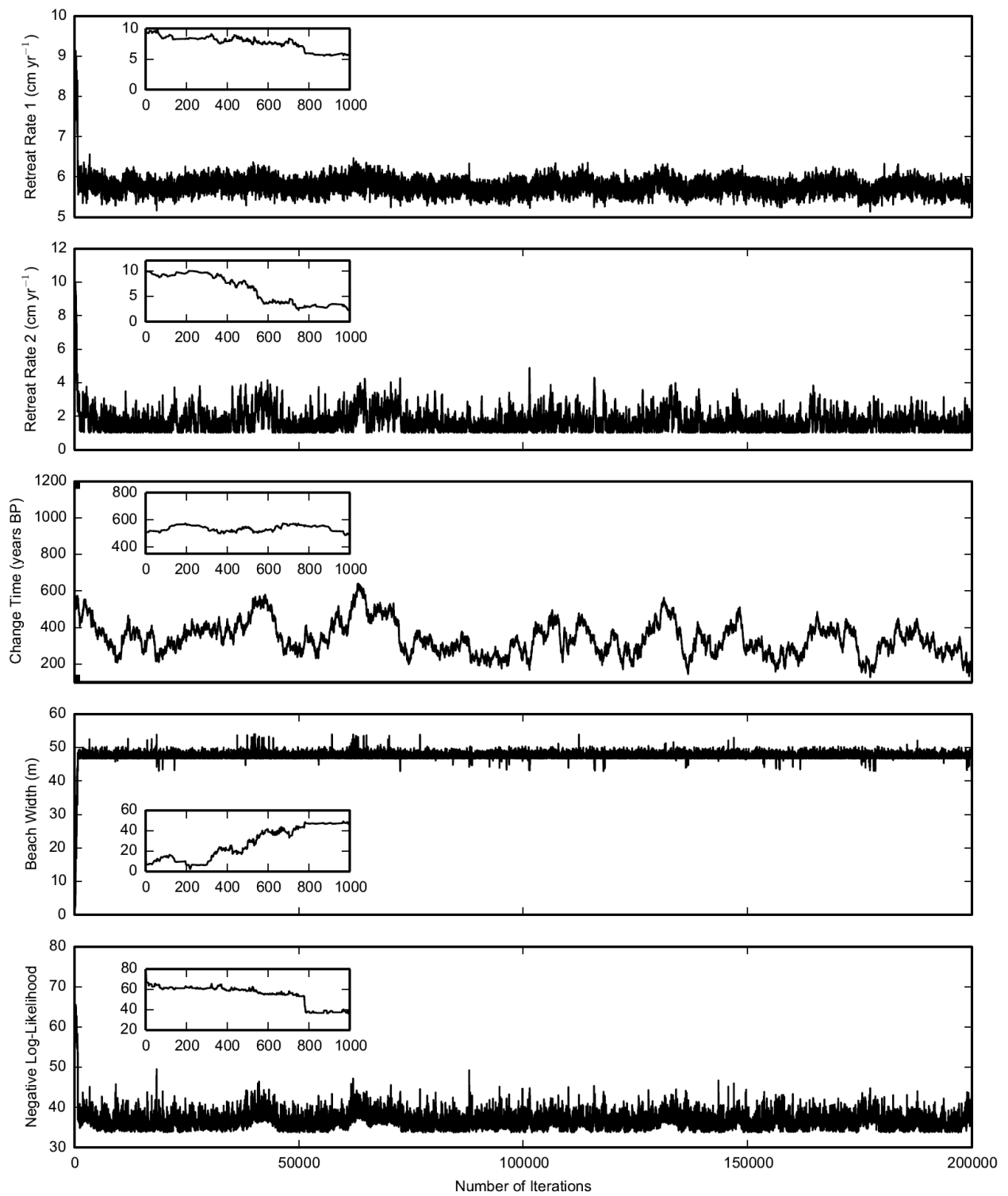


Figure S10: MCMC results for accepted parameters for Hope Gap using a step change retreat rate scenario. Inset plots show burn in period.

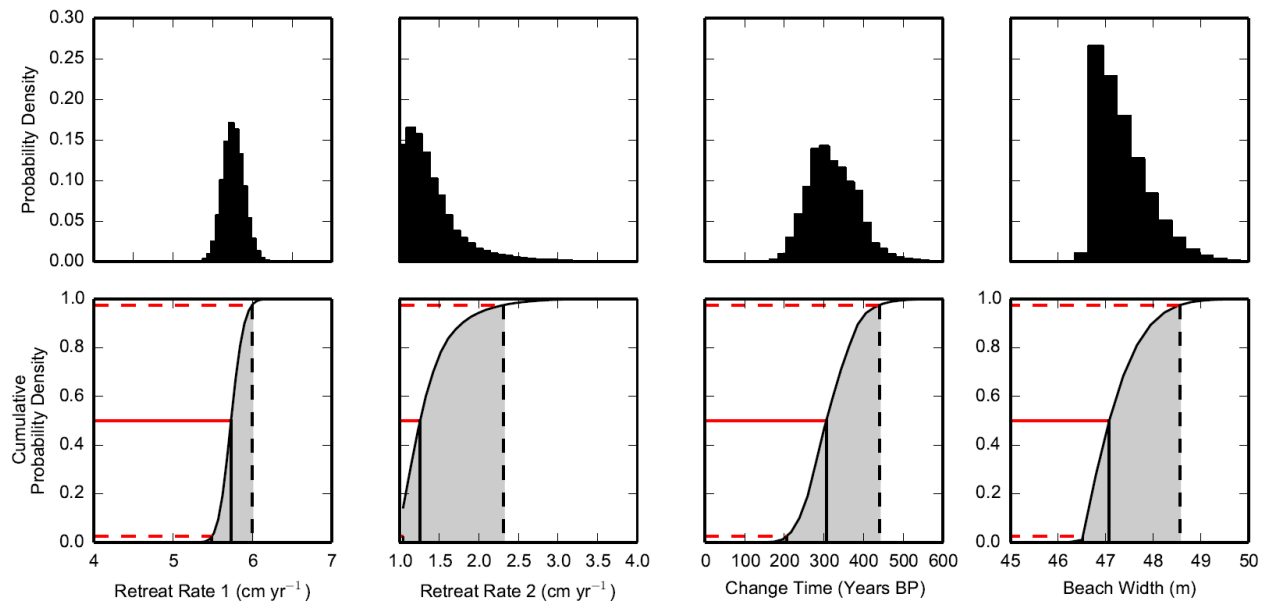


Figure S1 I: Likelihood weighted histograms giving parameter estimates for Hope Gap from MCMC inversion for a step change retreat rate scenario. Most likely values taken as the median with 95% confidence intervals. Note these plots include all data from Figure S10.

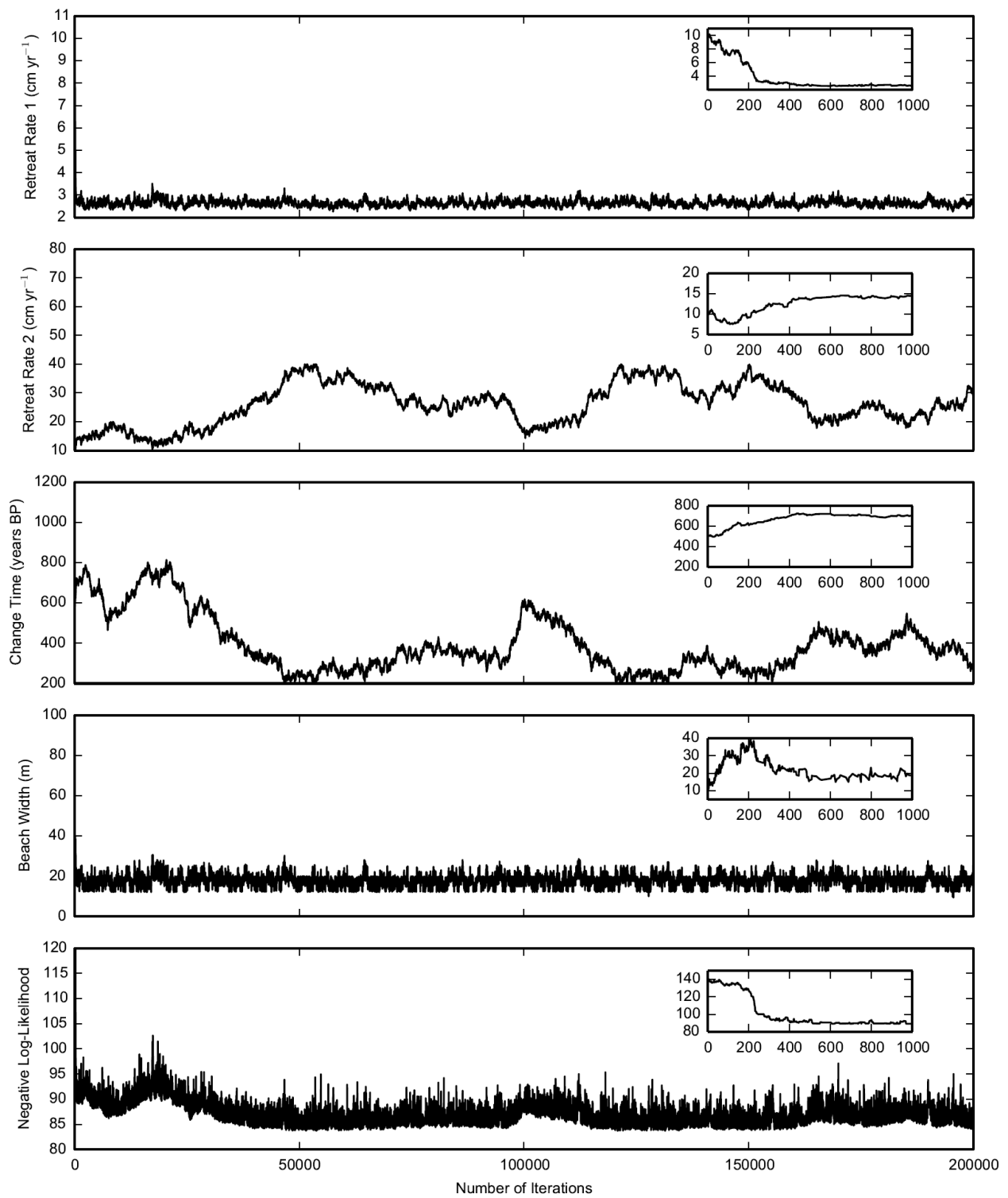


Figure S12: MCMC results for accepted parameters for Beachy Head using a step change retreat rate scenario. Inset plots show burn in period.

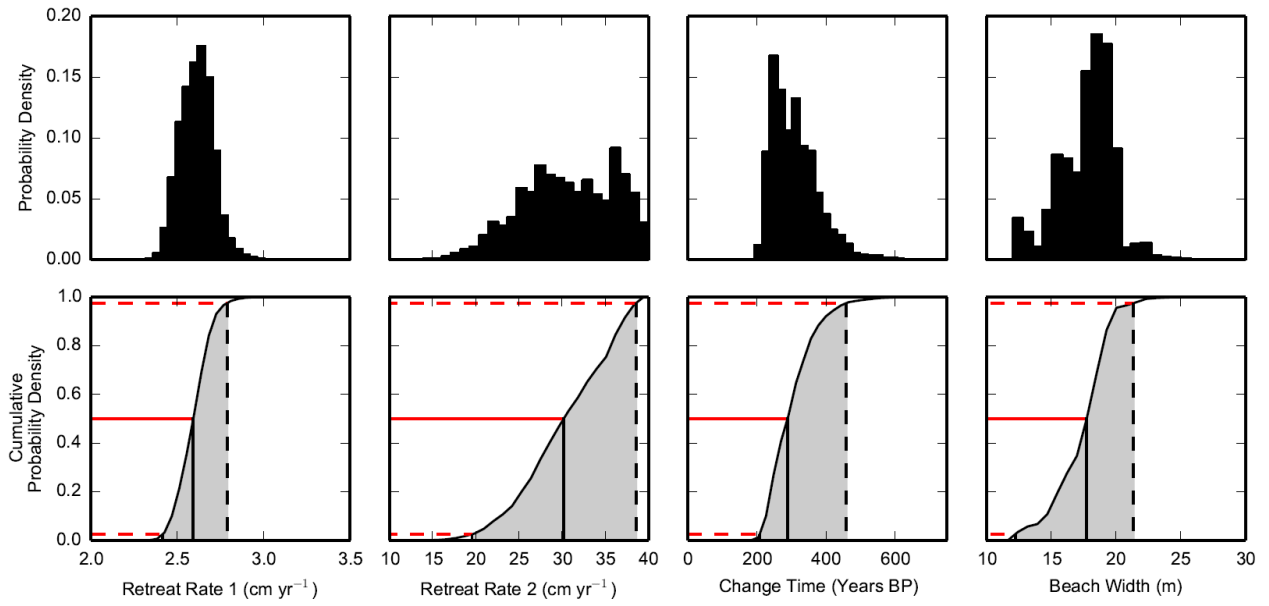


Figure S13: Likelihood weighted histograms giving parameter estimates for Beachy Head from MCMC inversion for a step change retreat rate scenario. Most likely values taken as the median with 95% confidence intervals. Note these plots include all data from Figure S11.

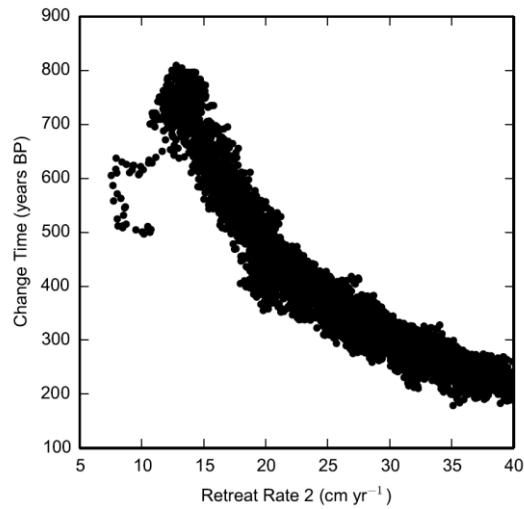


Figure S14: Plot of retreat rate 2 versus the timing of the change between retreat rate 1 and retreat rate 2. Negative correlation reflects trade off between the retreat rate 2 and change time such that a faster recent retreat rate does not need to have occurred as long ago to create the observed distribution of ^{10}Be concentrations.